NUMERICAL EVALUATION OF THE CENTERPLANE POTENTIAL OF A CENTERPLANE SOURCE DISTRIBUTION

by

F. Noblesse

The preparation of this report was
supported by a grant of the National
Science Foundation (Grant No. ENG75-03974)

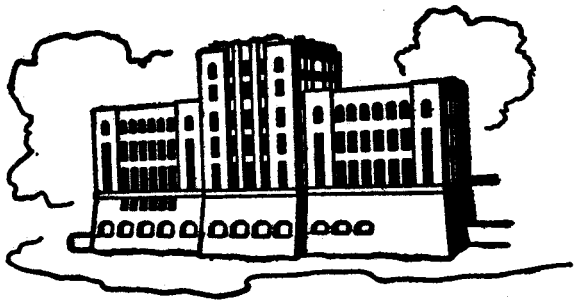

IIHR Report No. 179

Iowa Institute of Hydraulic Research
The University of Iowa
Iowa City, Iowa

August 1975

NUMERICAL EVALUATION OF THE CENTERPLANE POTENTIAL OF A CENTERPLANE SOURCE DISTRIBUTION

by

F. Noblesse

The preparation of this report was
supported by a grant of the National
Science Foundation (Grant No. ENG75-03974)

IIHR Report No. 179

Iowa Institute of Hydraulic Research
The University of Iowa
Iowa City, Iowa

August 1975

ABSTRACT

The paper is concerned with the development of a numerical procedure for evaluating the linearized velocity potential $\phi(x,y,o)$, on the plane z=0, for the steady free-surface gravity flow of a uniform stream past a given distribution of sources on the same plane z=0 assumed to be vertical and parallel to the oncoming stream (this plane z=0 is thus a plane of symmetry for the flow, which is referred to as the centerplane). The centerplane Havelock source potential is written in the form $G(x,y,o;\mu,\nu,o) = -1/r + Q(x',y')/r' + W(x',y')$ where r is the distance between the field point (x,y,o) and the source (μ,ν,o), $x' \equiv x-\mu$, $y' \equiv y+\nu$, $r' = (x'^2 + y'^2)^{\frac{1}{2}}$ is the distance between the field point and the image $(\mu,-\nu,o)$ of the source with respect to the free surface, and W(x',y') is the potential of the wave-like disturbance trailing behind the source. The strength of the image singularity Q(x',y') tends to +1 as $r' \to 0$ and to -1 as $r' \to \infty$. The numerical procedure is based on universal matrices which may be computed once and for all and stored on magnetic tape or disk.

ACKNOWLEDGEMENTS

The preparation of this report was supported by a grant of the National Science Foundation (Grant No.ENG75-03974). Additional funds for computer time were provided by the Graduate College of the University of Iowa. The author is grateful to both institutions for their support.

I also wish to thank Drs. Landweber, Dagan and Tatinclaux for their advice in the development of this numerical procedure.

LIST OF CONTENTS

		Page
I.	INTRODUCTION	1
II.	THE CENTERPLANE HAVELOCK SOURCE POTENTIAL	2
III.	THE CENTERPLANE POTENTIAL	6
IV.	OUTLINE OF FUTURE DEVELOPMENTS	11
Appendix 1.	Expression of the near-field disturbance in terms of the complex exponential integral	13
Appendix 2.	Numerical evaluation of the strength of the image singularity, $Q(x',y')$	14
Appendix 3.	Numerical evaluation of the wave integrals	16
REFERENCES		19
FIGURES		20

LIST OF FIGURES

Fig. 1	Definition sketch for the centerplane Havelock source potential	20
Fig. 2	Integration contours	20
Fig. 3	Strength of the image singularity	21
Fig. 4	Wave integrals	22

NUMERICAL EVALUATION OF THE CENTERPLANE POTENTIAL OF A CENTERPLANE SOURCE DISTRIBUTION

I. INTRODUCTION

The success enjoyed by Gadd [1] in predicting the "residuary resistance" of a number of ship hulls by the method of Guilloton [2], as well as studies by Dagan [3] and Noblesse [4] rationalizing Guilloton's method and suggesting possible modifications, have called for the development of a numerical procedure for evaluating the flow around a ship hull by a Guilloton-type method. The motivation for developing such a numerical procedure has recently been strengthened by further theoretical developments of Noblesse and Dagan [5] pointing to the possibility of obtaining a complete second-order thin-ship approximation by means of centerplane source distributions alone.

From the computational point of view, the essential feature of Guilloton's and related methods is that they involve source distributions on the ship centerplane alone, and furthermore that most quantities of practical interest, e.g., wave resistance, hydrodynamic lift and moment, sinkage and trim, velocity distribution on the hull and free-surface profile along the hull, can be obtained from flow variables evaluated at the centerplane. This means that the computational problem in these methods of evaluating the (three-dimensional) flow around a ship hull is two dimensional in nature, in that functions of two variables only need be evaluated, as will be shown below.

The velocity field in the centerplane, taken as the plane $z=0$, can be obtained by numerical differentiation of the centerplane velocity potential $\phi(x,y,0)$, and other quantities of interest such as the vertical

and longitudinal mapping functions (displacements) can likewise be easily derived from $\phi(x,y,0)$. The basic computational problem therefore consists in evaluating the centerplane velocity potential $\phi(x,y,0)$, simply denoted by $\phi(x,y)$ in the sequel, due to a given source distribution, of strength $\tau(x,y)$, on the centerplane z=0. The present report is then concerned with the numerical evaluation of the centerplane potential $\phi(x,y)$ given by

$$\phi(x,y) = \iint_{\sigma} G(x,y;\mu,\nu)\tau(\mu,\nu)d\mu d\nu \qquad (1.1)$$

where $G(x,y;\mu,\nu)$ denotes the centerplane Havelock source potential $G(x,y,0;\mu,\nu,0)$ and σ is a given area in the lower half plane $\nu\leq 0$ where the source distribution $\tau(\mu,\nu)$ is defined. The expression of $G(x,y;\mu,\nu)$, as well as the precise meaning of every symbol appearing in the above equation, is given in the sequel.

II. THE CENTERPLANE HAVELOCK SOURCE POTENTIAL

Let us consider the steady free-surface gravity flow of a uniform stream of velocity U past a unit source located at a point S below the free surface, see Fig. 1. The vertical plane passing through the source S and parallel to the oncoming stream U is a plane of symmetry for the flow. This plane is taken as the plane Z=0 and, in reference to the thin-ship theory, is referred to as the "centerplane". The horizontal undisturbed free surface is taken as the plane Y=0 with the Y axis directed upwards. The X axis is taken parallel to the oncoming uniform stream U and pointing downstream. The (dimensional) coordinates of the source S are denoted by $\{X_S, Y_S \leq 0, 0\}$ and the point P where the flow is observed has coordinates $\{X, Y \leq 0, 0\}$. The coordinates of the image S' of the source S with respect to the free surface are $\{X_S, -Y_S, 0\}$.

Variables are made dimensionless with respect to the acceleration of gravity g and the velocity U taken as reference quantities. Thus, dimensionless coordinates x,y,μ,ν are defined as

$$\{x,y,\mu,\nu\} = (g/U^2)\{X,Y,X_S,Y_S\} \tag{2.1}$$

The linearized velocity potential, on the centerplane z=0, for the flow described above is given by the "centerplane" Havelock source potential $G(x,y,0;\mu,\nu,0)$, which is simply denoted by $G(x,y;\mu,\nu)$ and is written in dimensionless form as

$$G(x,y;\mu,\nu) = -[(x-\mu)^2+(y-\nu)^2]^{-1/2} + R(x-\mu,y+\nu) \tag{2.2}$$

where $R(x-\mu,y+\nu)$ is a function of the two variables $x-\mu$ and $y+\nu$ defined - and regular - in the lower half space $y+\nu<0$. We have

$$R(x-\mu,y+\nu) = [(x-\mu)^2+(y+\nu)^2]^{-1/2} + \frac{4}{\pi}\int_0^{\pi/2}\int_0^{\infty} \frac{e^{k[(y+\nu)+i(x-\mu)\cos\theta]}}{k\cos^2\theta-1}\,dk\,d\theta$$

$$+ 4i\int_0^{\pi/2} e^{[(y+\nu)+i(x-\mu)\cos\theta]\sec^2\theta}\sec^2\theta\,d\theta \tag{2.3}$$

where the convention is made that only the real part of the right-hand side is to be taken. Equation (2.3) can easily be derived from eq. (13.36) p. 485 in Wehausen [6] (it must be remembered that the equation given by Wehausen holds for the case of a uniform stream flowing past a sink in the negative x direction).

Let us introduce the complex number ζ defined by

$$\zeta = (y+\nu)\sec^2\theta + i(x-\mu)\sec\theta \tag{2.4}$$

Eq. (2.3) can then be written as

$$R(x-\mu,y+\nu) = [(x-\mu)^2+(y+\nu)^2]^{-1/2} + \frac{4}{\pi}\int_0^{\pi/2} I(\zeta)\sec^2\theta\,d\theta + 4i\int_0^{\pi/2} e^{\zeta}\sec^2\theta\,d\theta \tag{2.5}$$

where the change of variable $k=\gamma \sec^2\theta$ was performed in the double integral, with $I(\zeta)$ defined as

$$I(\zeta) = \int_0^\infty \frac{e^{\gamma\zeta}}{\gamma-1}\, d\gamma \tag{2.6}$$

The Cauchy-principal-value integral $I(\zeta)$ can be written in terms of the complex exponential integral $E_1(\zeta)$, see Appendix 1. It yields

$$I(\zeta) = e^{\zeta} E_1(\zeta) + i\pi \operatorname{sgn}(x-\mu) e^{\zeta} \tag{2.7}$$

where $\operatorname{sgn}(x-\mu)=(x-\mu)/|x-\mu|$ and

$$E_1(\zeta) = \int_\zeta^\infty \frac{e^{-t}}{t}\, dt \qquad (|\arg\zeta|<\pi) \tag{2.8}$$

as defined in eq. (5.1.1) p. 228 in Abramowitz and Stegun [7].

By using eq. (2.7), eq. (2.5) can be written as

$$R(x-\mu,y+\nu) = N(x-\mu,y+\nu) + W(x-\mu,y+\nu) \tag{2.9}$$

where $N(x-\mu,y+\nu)$ and $W(x-\mu,y+\nu)$ are defined as

$$N(x-\mu,y+\nu) = [(x-\mu)^2+(y+\nu)^2]^{-1/2} + \frac{4}{\pi}\int_0^{\pi/2} e^{\zeta} E_1(\zeta) \sec^2\theta\, d\theta \tag{2.10}$$

$$W(x-\mu,y+\nu) = 8iH(x-\mu)\int_0^{\pi/2} e^{\zeta}\sec^2\theta\, d\theta \tag{2.11}$$

In eq. (2.11), $H(x-\mu)$ is the Heaviside step function defined as $H(x-\mu)=0$ for $x<\mu$ and $H(x-\mu)=1$ for $x>\mu$. Only the real parts of the right-hand sides of eqs. (2.10) and (2.11) are to be taken, in accordance with the convention adopted in eq. (2.3). It is easily seen that $N(\mu-x,y+\nu) = N(x-\mu,y+\nu)$ so that this term represents a disturbance symmetric upstream and downstream from the source. Furthermore, $N(x-\mu,y+\nu)$ represents a nonoscillatory "near-field disturbance", as shown below. The term $W(x-\mu,y+\nu)$, on the other hand, is zero upstream from the source and represents an oscillatory wave-like disturbance. In particular, far downstream from the

source, $W(x-\mu,y+\nu)$ behaves like

$$W(x-\mu,y+\nu) \sim -8(\pi/2)^{1/2} e^{y+\nu}(x-\mu)^{-1/2}\sin(x-\mu+\pi/4) \qquad (x-\mu>>1)$$

as can readily be obtained by the method of stationary phase. Hereafter, the terms $N(x-\mu,y+\nu)$ and $W(x-\mu,y+\nu)$ are referred to as the "near-field" and "wave" terms, respectively.

A good picture of the behavior of the near-field term $N(x-\mu,y+\nu)$ is obtained by writing it as follows:

$$N(x-\mu,y+\nu) = Q(x-\mu,y+\nu)[(x-\mu)^2+(y+\nu)^2]^{-1/2} \tag{2.12}$$

where $Q(x-\mu,y+\nu)$ is defined as

$$Q(x-\mu,y+\nu) = 1 + \frac{4}{\pi}[(x-\mu)^2+(y+\nu)^2]^{1/2}\int_0^{\pi/2} \mathrm{Re}\{e^{\zeta}E_1(\zeta)\}\sec^2\theta d\theta \tag{2.13}$$

The function $Q(x-\mu,y+\nu)$ has been evaluated numerically, see Appendix 2, and is represented in Fig. 3 for $0\leq x-\mu\leq 3$, $0\geq y+\nu\geq -3$. It is seen in Fig. 3 that $Q(x-\mu,y+\nu)\to 1$ as $r'\equiv[(x-\mu)^2+(y+\nu)^2]^{\frac{1}{2}}\to 0$. On the other hand, $Q(x-\mu,y+\nu)\to -1$ as $r'\to\infty$, as one readily obtains by substituting $e^{\zeta}E_1(\zeta)$ in eq. (2.13) by the first term, i.e., $1/\zeta$, in the asymptotic expansion of $e^{\zeta}E_1(\zeta)$ for $|\zeta|>>1$, see eq. (5.1.51) p. 231 in Abramowitz and Stegun [7]. Keeping two more terms in this asymptotic expansion, i.e., taking $e^{\zeta}E_1(\zeta)\sim 1/\zeta-1/\zeta^2+2/\zeta^3$, yields

$$Q(x',y')\sim -1+\frac{2}{r'}\left(\frac{y'}{r'}+\frac{1}{1-y'/r'}\right) - \frac{6}{r'^2}\frac{y'}{r'}\left(\frac{y'}{r'}+\frac{2-y'/r'}{(1-y'/r')^2}\right) \qquad (r'>>1) \tag{2.14}$$

where $x'\equiv x-\mu$, $y'\equiv y+\nu$, and $r'=(x'^2+y'^2)^{1/2}$ as already defined above.

In summary, by using (2.2), (2.9) and (2.12), the centerplane Havelock source potential $G(x,y;\mu,\nu)$ can be written in the form

$$G(x,y;\mu,\nu) = -\frac{1}{r} + \frac{Q(x',y')}{r'} + W(x',y') \tag{2.15}$$

where $r\equiv[(x-\mu)^2+(y+\nu)^2]^{1/2}$, and $Q(x',y')$ and $W(x',y')$ are given by (2.13) and (2.11), respectively. Thus, the velocity potential of a submerged

source in an oncoming uniform stream is written as the sum of three terms: (i) the potential $-1/r$ of the source in an infinite domain, (ii) the near-field disturbance potential $Q(x',y')/r'$ which may be interpreted as the potential of an image sink of strength $Q(x',y')$ in an infinite domain, and (iii) the potential $W(x',y')$ of the wave-like disturbance trailing behind the source. It is convenient to refer to the function $Q(x',y')$ as the "strength of the image singularity". Since $Q \to -1$ as $r' \to \infty$ (i.e., as the field point is very far from the source) and $Q \to +1$ as $r' \to 0$ (i.e., as the source and the field point approach each other and the free surface), the "image singularity" of a unit source is seen to become a unit source or sink as $r' \to \infty$ or $r' \to 0$, respectively.

III. THE CENTERPLANE POTENTIAL

We start by defining notations which are used in several instances in the present section. Let a continuous function $f(x,y)$ be given. We define four functions $f^{pq}(x,y;h,k)$, $(p,q=0,1)$ in terms of the values of $f(x,y)$ at the points $x \pm h$, $y \pm k$ by the following expressions

$$
\begin{aligned}
4f^{00}(x,y;h,k) &= f(x+h,y+k) + f(x-h,y+k) \\
&\quad + f(x-h,y-k) + f(x+h,y-k) \\
4hf^{10}(x,y;h,k) &= [f(x+h,y+k)-f(x-h,y+k)] \\
&\quad + [f(x+h,y-k)-f(x-h,y-k)] \\
4kf^{01}(x,y;h,k) &= [f(x+h,y+k)-f(x+h,y-k)] \\
&\quad + [f(x-h,y+k)-f(x-h,y-k)] \\
4hkf^{11}(x,y;h,k) &= [f(x+h,y+k)+f(x-h,y-k)] \\
&\quad - [f(x-h,y+k)+f(x+h,y-k)]
\end{aligned}
\tag{3.1}
$$

It is readily seen that $f^{00}(x,y;h,k)$ represents an average value of the function $f(x,y)$ over the rectangle $x-h \leq x \leq x+h$, $y-k \leq y \leq y+k$, while f^{10} and f^{01} are average slopes in the x and y directions, respectively, and f^{11} gives an average value of the second partial derivative f_{xy}.

We now proceed with the proper subject of the present section, which is the numerical evaluation of the centerplane potential $\phi(x,y)$ defined in eq. (1.1). Let the centerplane Green function $G(x,y;\mu,\nu)$ be written in the form $G(x-\mu,y\pm\nu)$. The centerplane potential $\phi(x,y)$ is then given by

$$\phi(x,y) = \iint_{\sigma} G(x-\mu,y\pm\nu)\,\tau(\mu,\nu)\,d\mu d\nu \tag{3.2}$$

$\phi(x,y)$ is to be evaluated at the nodes of a rectangular numerical mesh $x_1<x_2<\ldots<x_m<\ldots<x_{M+1}$ and $y_1=0>y_2>\ldots>y_n>\ldots>y_{N+1}$. The value of $\phi(x,y)$ at the node $x=x_m$, $y=y_n$ is given by

$$\phi(x_m,y_n) = \sum_{i=1}^{M} \sum_{j=1}^{N} \phi_{ijmn} \tag{3.3}$$

where ϕ_{ijmn} is defined by

$$\phi_{ijmn} = \int_{x_i}^{x_{i+1}} d\mu' \int_{y_{j+1}}^{y_j} d\nu'\; G(x_m-\mu',y_n\pm\nu')\;\tau(\mu',\nu') \tag{3.4}$$

We introduce the quantities $\bar{x}_i$, $\bar{y}_j$, h_i and k_j defined as

$$\begin{aligned} \bar{x}_i &= (x_i+x_{i+1})/2,\quad \bar{y}_j = (y_j+y_{j+1})/2 \\ h_i &= (x_{i+1}-x_i)/2,\quad k_j = (y_j-y_{j+1})/2 \end{aligned} \tag{3.5}$$

With $\mu' = \bar{x}_i+\mu$ and $\nu' = \bar{y}_j+\nu$, eq. (3.4) then becomes

$$\phi_{ijmn} = \int_{-h_i}^{h_i} d\mu \int_{-k_j}^{k_j} d\nu\; G(x_m-\bar{x}_i-\mu,y_n\pm\bar{y}_j\pm\nu)\;\tau(\bar{x}_i+\mu,\bar{y}_j+\nu) \tag{3.6}$$

In each rectangle $-h_i \leq \mu \leq h_i$, $-k_j \leq \nu \leq k_j$, the source density function $\tau(\bar{x}_i+\mu,\bar{y}_j+\nu)$ is approximated by

$$\tau(\bar{x}_i+\mu,\bar{y}_j+\nu) = \sum_{p=0}^{1}\sum_{q=0}^{1} \tau^{pq}(\bar{x}_i,\bar{y}_j;h_i,k_j)\mu^p\nu^q \tag{3.7}$$

where the four coefficients $\tau^{pq}(\bar{x}_i,\bar{y}_j;h_i,k_j)$ are related to the values of the source density function $\tau(\bar{x}_i\pm h_i,\bar{y}_j\pm k_j)$ at the corners of the rectangle by means of eqs. (3.1)

We introduce the following notations

$$x_{mi} = x_m-\bar{x}_i,\ y_{nj} = y_n-\bar{y}_j,\ y'_{nj} = y_n+\bar{y}_j \tag{3.8}$$

We also define the quantities

$$S_{pq}(x_{mi},y_{nj};h_i,k_j) = \int_{h_i}^{h_i}d\mu\int_{k_j}^{k_j}d\nu[(x_{mi}-\mu)^2 + (y_{nj}-\nu)^2]^{-1/2}\mu^p\nu^q \tag{3.9}$$

$$N_{pq}(x_{mi},y'_{nj};h_i,k_j) = \int_{h_i}^{h_i}d\mu\int_{k_j}^{k_j}d\nu N(x_{mi}-\mu,y'_{nj}+\nu)\mu^p\nu^q \tag{3.10}$$

$$W_{pq}(x_{mi},y'_{nj};h_i,k_j) = \int_{h_i}^{h_i}d\mu\int_{k_j}^{k_j}d\nu W(x_{mi}-\mu,y'_{nj}+\nu)\mu^p\nu^q \tag{3.11}$$

where $N(x_{mi}-\mu,y'_{nj}+\nu)$ and $W(x_{mi}-\mu,y'_{nj}+\nu)$ have been defined in eqs. (2.10) and (2.11). Eqs. (2.2), (2.9) and (3.7)-(3.11) show that eq. (3.6) becomes

$$\phi_{ijmn} = \sum_{p=0}^{1}\sum_{q=0}^{1} \tau^{pq}(\bar{x}_i,\bar{y}_j;h_i,k_j)\phi^{pq}_{ijmn} \tag{3.12}$$

where ϕ^{pq}_{ijmn} is defined by

$$\phi^{pq}_{ijmn} = -S_{pq}(x_{mi},y_{nj};h_i,k_j) + N_{pq}(x_{mi},y'_{nj};h_i,k_j) + W_{pq}(x_{mi},y'_{nj};h_i,k_j) \tag{3.13}$$

Closed-form analytical expressions for the "source terms" $S_{pq}(x_{mi},y_{nj};h_i,k_j)$ can easily be obtained. The "near-field terms" $N_{pq}(x_{mi},y'_{nj};h_i,k_j)$ can be expressed in terms of the "source terms" $S_{pq}(x_{mi},y'_{nj};h_i,k_j)$ by writing the near-field disturbance $N(x_{mi}-\mu,y'_{nj}+\nu)$ as in eq. (2.12), and approximating the function $Q(x_{mi}-\mu,y'_{nj}+\nu)$ by

$$Q(x_{mi}-\mu,y'_{nj}+\nu) = \sum_{r=0}^{1}\sum_{s=0}^{1} (-1)^r Q^{rs}(x_{mi},y'_{nj};h_i,k_j)\mu^r\nu^s \tag{3.14}$$

in each rectangle $-h_i\leq\mu\leq h_i$, $-k_j\leq\nu\leq k_j$. The coefficients $Q^{rs}(x_{mi},y'_{nj};h_i,k_j)$

are related to the values of the function $Q(x_{mi}\pm h_i, y'_{nj}\pm k_j)$ at the corners of the rectangle by means of eqs. (3.1). The "near-field terms" $N_{pq}(x_{mi}, y'_{nj}; h_i, k_j)$ then become

$$N_{pq}(x_{mi}, y'_{nj}; h_i, k_j) =$$
$$\sum_{r=0}^{1}\sum_{s=0}^{1} (-1)^r Q^{rs}(x_{mi}, y'_{nj}; h_i, k_j)\ S_{p+r,q+s}(x_{mi}, y'_{nj}; h_i, k_j) \tag{3.15}$$

These "near-field terms" can thus simply be expressed in terms of the "strength of the image singularity" $Q(x', y')$ and the nine quantities

$$S_{\alpha\beta}(x,y;h,k) = \int_{-h}^{h} d\mu \int_{-k}^{k} d\nu [(\mu-x)^2+(\nu-y)^2]^{-\frac{1}{2}}\ \mu^\alpha \nu^\beta; \quad (\alpha,\beta=0,1,2) \tag{3.16}$$

which can be written in closed-form analytical expressions.

For $|x_{mi}| \geq h_i$, eqs. (2.11) and (3.11) yield

$$W_{pq}(x_{mi}, y'_{nj}; h_i, k_j) = 8i\ H(x_{mi}) \int_0^{\pi/2} I_{pq}(\theta; x_{mi}, y'_{nj}, h_i, k_j)\ \sec^2\theta d\theta \tag{3.17}$$

where the quantity $I_{pq}(\theta;x,y,h,k)$ is defined by

$$I_{pq}(\theta;x,y,h,k) = \int_{-h}^{h} e^{-i(\mu-x)\sec\theta} \mu^p d\mu \int_{-k}^{k} e^{(\nu+y)\sec^2\theta} \nu^q d\nu \tag{3.18}$$

It is emphasized that eq. (3.17) is not valid for $|x_{mi}| < h_i$. One easily obtains

$$\begin{aligned}
I_{00} &= i\cos^3\theta\{e^{(y+\nu)\sec^2\theta + i(x-\mu)\sec\theta}\}_{-h,-k}^{h,k} \\
I_{10} &= i\cos^3\theta\{e^{(y+\nu)\sec^2\theta + i(x-\mu)\sec\theta}(\mu - i\cos\theta)\}_{-h,-k}^{h,k} \\
I_{01} &= i\cos^3\theta\{e^{(y+\nu)\sec^2\theta + i(x-\mu)\sec\theta}(\nu - \cos^2\theta)\}_{-h,-k}^{h,k} \\
I_{11} &= i\cos^3\theta\{e^{(y+\nu)\sec^2\theta + i(x-\mu)\sec\theta}(\mu - i\cos\theta)(\nu - \cos^2\theta)\}_{-h,-k}^{h,k}
\end{aligned} \tag{3.19}$$

where the arguments of $I_{pq}(\theta;x,y,h,k)$ have been omitted for shortness.

We introduce the quantity $\Omega_p(x,y) = \Omega c_p(x,y) + i\,\Omega s_p(x,y)$ defined as

$$\Omega_p(x,y) = \Omega c_p(x,y) + i\,\Omega s_p(x,y) = \int_0^{\pi/2} e^{y\sec^2\theta + ix\sec\theta} \cos^p\theta d\theta \tag{3.20}$$

where $y \leq 0$, $x \geq 0$ and $p \geq 1$. Equations (3.17), (3.18) and (3.19) then give

$$
\begin{aligned}
W_{00}(x_{mi},y'_{nj};h_i,k_j) &= 32h_ik_j\ H(x_{mi})\ \Omega c_1^{11}(x_{mi},y'_{nj};h_i,k_j)\\
W_{10} &= 32h_ik_j\ H(x_{mi})(-\Omega c_1^{01}+\Omega s_2^{11})\\
W_{01} &= 32h_ik_j\ H(x_{mi})(\Omega c_1^{10}-\Omega c_3^{11})\\
W_{11} &= 32h_ik_j\ H(x_{mi})(\Omega c_1^{00}+\Omega s_2^{10}+\Omega c_3^{01}-\Omega s_4^{11})
\end{aligned}
\qquad (3.21)
$$

where the notations defined in eqs. (3.1) have been used. Thus, the "wave terms" $W_{pq}(x_{mi},y'_{nj};h_i,k_j)$ are expressed simply in terms of the four integrals Ωc_1, Ωs_2, Ωc_3 and Ωs_4. These integrals are referred to as the "wave integrals", and are examined in Appendix 3.

In summary, the centerplane potential $\phi(x_m,y_n)$ is given by eqs. (3.3), (3.12), (3.13), (3.15) and (3.21). These equations involve the following basic quantities: the "strength of the image singularity" $Q(x-\mu,y+\nu)$ defined in eq. (2.13), the nine "source terms" $S_{\alpha\beta}(x,y;h,k)$ defined in eq. (3.16) and the four "wave integrals" $\Omega_p(x,y)$ defined in eq. (3.20). The numerical evaluation of the functions $Q(x-\mu,y+\nu)$ and $\Omega_p(x,y)$ is discussed in Appendices 2 and 3, respectively.

A similar numerical procedure has previously been developed by Yeung [8] for the calculation of sinkage and trim. The present procedure follows closely Yeung with respect to the treatment of the "wave disturbance" (the wave integrals $\Omega_p(x,y)$ defined in (3.20) are identical to Yeung's $J^{c,s}_{P+1}$ integrals), but the "near field disturbance" is treated somewhat differently.

IV. OUTLINE OF FUTURE DEVELOPMENTS

The present stage of development of the numerical procedure is essentially as described in this report, with the strength of the image singularity, $Q(x-\mu,y+\nu)$, and the wave integrals $\Omega c_1(x-\mu,y+\nu)$, Ωs_2, Ωc_3 and Ωs_4 evaluated at a sufficient number of points $(x-\mu, y+\nu)$ for these functions to be defined with accuracy 10^{-6} by means of a bicubic spline interpolator routine. The computed values of Q and of the four wave integrals are stored on a magnetic tape.

One way, probably the shortest way, from this stage on,would be to select a constant-size rectangular numerical mesh, i.e., $h_i \equiv h$ for $i = 1,2,\ldots,M$ and $k_j \equiv k$ for $j = 1,2,\ldots,N$, and form the eight matrices $N_{pq}(x_{mi},y'_{nj};h,k)$ and $W_{pq}(x_{mi},y'_{nj};h,k)$,$(p,q = 0,1)$ defined in eqs. (3.15) and (3.21). For given values of h and k, these matrices are universal, and thus need be constructed once and for all, then stored on a magnetic tape (if desired, the four matrices $S_{pq}(x_{mi},y_{nj};h,k)$ can also be evaluated and stored on a tape). With these matrices formed, the evaluation of the potential $\phi(x_m,y_n)$ at any mode (x_m,y_n) of the numerical mesh amounts to simple additions to be performed by the computer, as shown by eqs. (3.3), (3.12) and (3.13).

In order to cover the range of Froude numbers of practical interest, say $0.1 \leq F_r \leq 1$, several values of h and k must be considered. It would seem sufficient to consider four cases, and thus four sets of matrices: (i) $h = 0.025$, $k = 0.0125$ for $0 \leq x' \leq 5$, $0 \geq y' \geq -1$, (ii) $h = 0.05$, $k = 0.025$ for $0 \leq x' \leq 10$, $0 \geq y' \geq -2$, (iii) $h = 0.1$, $k = 0.05$ for $0 \leq x' \leq 20$, $0 \geq y' \geq -4$, and (iv) $h = k = 0.1$ for smaller Froude numbers. This represents fairly large matrices, containing some 16,000 elements each.

The size of these matrices appears to be too large for direct storage in the memory of the computer (for a given Froude number, hence for given h and k, eight or twelve of these matrices should be stored in the memory of the computer, as discussed above). For permanent record, these matrices would be stored on magnetic tape, and temporary storage on disk could be used for the purpose of numerical calculations.

Although the procedure described above should be feasible, the access time from the disk to the computer might be significant. In addition, this procedure is somewhat rigid due to the fixed-size uniform numerical mesh. It may thus be worthwhile to develop asymptotic expansions and rational approximations for the near-field disturbance $N(x-\mu,y+\nu)$ and the four wave integrals. Figure 3 and eqs. (2.12) and (2.14) suggest that the function $N(x',y')$ should be written as

$$N(x',y') = \begin{cases} 1/r' + f_o(y'/r') + r' f_1(y'/r', r') & \text{for } r' \text{ small} \\ \\ -1/r' + \sum_{k=1}^{n} a_k(y'/r')/r'^k & \text{for } r' \text{ large} \end{cases}$$

where $a_k(y'/r')$ are the functions appearing in the asymptotic expansion of $N(x',y')$ for large r', as in eq. (2.14), and $f_o(y'/r')$ and $f_1(y'/r')$ denote functions of y'/r'. A preliminary analysis shows that four or five additional terms in the asymptotic expansion (2.14) would yield an approximation to the near-field disturbance $N(x',y')$ with errors less than 10^{-6} for $r' > 20$ or even 15. Asymptotic expansions for the wave integrals can be obtained by the methods of stationary phase or steepest descent.

Appendix 1. Expression of the near-field disturbance in terms of the complex exponential integral

Let the complex number ζ, defined in eq. (2.4), be written in the polar form $\zeta=ae^{i\alpha}$, where $a\geq 0$ and $\pi/2\leq\alpha\leq 3\pi/2$ since $y+\nu\leq 0$ and $x-\mu\gtrless 0$. Following Hess and Smith [9] and others, see Yeung [8], the Cauchy pincipal value integral $I(\zeta)$, defined in eq. (2.6), can be expressed as the sum of an oscillatory term and a nonoscillatory term by means of an appropriate contour integration in the complex γ plane. Let the complex variable γ be written in the polar form $\gamma=\rho e^{i\psi}$. We then have $\gamma\zeta=a\rho e^{i(\alpha+\psi)}$. The exponential term $e^{\gamma\zeta}$ in the integral (2.6) can be rendered monotonic decreasing by choosing $\psi=\pi-\alpha$, which yields $\gamma\zeta=-a\rho$. Performing the contour integrations shown in Fig. 2 then yields

$$\oint_0^\infty \frac{e^{\gamma\zeta}}{\gamma-1}\,d\gamma \mp i\pi e^{\zeta} + \int_\infty^0 \frac{e^{-a\rho}}{\rho e^{i(\pi-\alpha)}-1}\,e^{i(\pi-\alpha)}\,d\rho = 0$$

where the - and + signs correspond to the upper and lower contours (case $x-\mu>0$ and $x-\mu<0$), respectively. This readily gives

$$I(\zeta) = \pm i\pi e^{\zeta} + \int_0^\infty \frac{e^{-a\rho}}{\rho+e^{i\alpha}}\,d\rho$$

Equation (2.7) is finally obtained by successively performing the change of variables $\lambda=a\rho$ and $t=\lambda+\zeta$ in the above integral.

Appendix 2. Numerical evaluation of the strength of the image singularity

For simplicity, we use the notations $x'=x-\mu$, $y'=y+\nu$ already introduced in Section II. The complex number ζ defined in eq. (2.4) then becomes $\zeta = y'\sec^2\theta + i\, x'\sec\theta$, where $y' \leq 0$. We have $e^{\bar{\zeta}}E_1(\bar{\zeta}) = \overline{e^{\zeta}E_1(\zeta)}$, see Abramowitz and Stegun [7] p. 229, and eq. (2.13) then readily shows that $Q(-x',y') = Q(x',y')$. The numerical evaluation of $Q(x',y')$ may thus be restricted to $x' \geq 0$, $y' \leq 0$.

As θ increases from 0 to $\pi/2$, the point ζ moves along the parabola $\zeta_r = (y'/x'^2)\zeta_i^2$ from $\zeta_o = y' + ix'$ to infinity, in the second quadrant of the complex plane $\zeta = \zeta_r + i\zeta_i = y'\sec^2\theta + i\, x'\sec\theta$. The rate at which ζ moves along this parabola, given by $d\zeta/d\theta$, depends on $y'+ix'$. In particular, $d\zeta/d\theta \to 0$ as $y' + ix' \to 0$.

Performing the change of variable $t = c \tan\theta$, with c an arbitrary constant, in eq. (2.13) yields

$$Q(x',y') = 1 + \frac{4}{\pi}\frac{r'}{c}\int_0^{\infty} \mathrm{Re}\{e^{\zeta}E_1(\zeta)\}\, dt \qquad \text{(A2.1)}$$

where $\zeta = -\beta(t^2+c^2) + i\alpha(t^2+c^2)^{1/2}$ with $\alpha = x'/c$ and $\beta = -y'/c^2$. The efficiency of the numerical evaluation of the above integral was greatly improved by using the asymptotic expansion of $e^{\zeta}E_1(\zeta)$, see eq. (5.1.51) p. 231 in Abramowitz and Stegun [7]. The first three terms in this asymptotic expansion were retained and Eq. (A2.1) was written as

$$Q(x',y') \simeq 1 + \frac{4}{\pi}\frac{r'}{c}\int_0^{t_o} \mathrm{Re}\{e^{\zeta}E_1(\zeta)\}\, dt + \frac{4}{\pi}\frac{r'}{c}\int_{t_o}^{\infty} \mathrm{Re}\{\frac{1}{\zeta} - \frac{1}{\zeta^2} + \frac{2}{\zeta^3}\}\, dt \qquad \text{(A2.2)}$$

A closed-form analytical expression was developed for the last integral (the asymptotic expansion (2.14) was obtained from this expression by setting $t_o = 0$). The value of t_o was so chosen as to yield $Q(x',y')$ with

an error less than 10^{-6}.

The first integral in eq. (A2.2) was evaluated numerically. Simpson's integration rule was used; the specified accuracy was 5.10^{-7}. The integrand $e^{\zeta}E_1(\zeta)$ was evaluated by means of the rational approximation developed by Hershey [10], supplemented by the asymptotic expansion (5.1.51) in Abramowitz and Stegun, for large values of $|\zeta|$. The values of the exponential integral obtained by using Hershey's rational approximation were checked against the values given by Abramowitz and Stegun [7]. The specified accuracy for the integrand $e^{\zeta}E_1(\zeta)$ was 10^{-8}. For the numerical integration of the first integral in eq. (A2.2), it was found convenient to select the constant c as c=r'/(5+r'), which remedies the difficulty mentioned above, i.e., that the rate at which the point ζ moves along the parabola $\zeta_r=(y'/x'^2)\zeta_i^2$ vanishes as $\zeta\to 0$, and yields a relatively uniform value for the upper limit of integration t_o (t_o varies between 4 and 20, the higher values being attained for smaller values of y' and r'). The computing time on the IBM 360/65 at the computer center of the University of Iowa varied between 0.1 sec to 1 sec per value of Q(x',y') depending on x' and y', the computing time increasing fairly rapidly as $r'\to 0$. This represented a cost varying between less than 1¢ up to about 8¢ per value of the function Q.

Appendix 3. Numerical evaluation of the wave integrals

For the purpose of numerical integration, the change of variable $\sinh t = \tan \theta$ was performed in the wave integral (3.20) which was then written as

$$\Omega_p(x,y) = e^{ix} \int_0^\infty \frac{e^{y \cosh^2 t}\, e^{ix(\cosh t - 1)}}{\cosh^{p+1} t}\, dt$$

The integrand in the above integral is the product of two monotonic decreasing functions, namely $\exp(y \cosh^2 t)$ and $\operatorname{sech}^{p+1} t$, and the oscillatory function $\exp[ix(\cosh t - 1)]$. Each of these three functions depends on one parameter only, i.e., $y \leq 0$, $p \geq 1$ and $x \geq 0$, respectively. It is readily seen that $\exp(y \cosh^2 t) \leq \varepsilon_y$ if $t \geq t_y$ where $t_y = \cosh^{-1}[(\log \varepsilon_y)/y]^{\frac{1}{2}}$. Similarly, $\operatorname{sech}^{p+1} t \leq \varepsilon_p$ if $t \geq t_p = \cosh^{-1}[(1/\varepsilon_p)^{1/(p+1)}]$. Finally, the k^{th} oscillation of the oscillatory function $\exp[ix(\cosh t - 1)]$ occurs at $t = t_{x,k} = \cosh^{-1}(1 + 2k\pi/x)$, $k = 1,2,\ldots$

It is then easily seen that $t_y \leq t_p$ if $y \leq \varepsilon_p^{2/(p+1)} \log \varepsilon_y$. This shows that - except for $y = 0$ - the function $\exp(y \cosh^2 t)$ may be considered the fastest decreasing function. Next, by comparing $t_{x,k}$ and t_y, it is found that $\exp[ix(\cosh t - 1)]$ undergoes at least 5 oscillations ($k = 5$) before $\exp(y \cosh^2 t)$ decreases to 10^{-7} ($\varepsilon_y = 10^{-7}$) if $x > 10\pi/[4(-y)^{-\frac{1}{2}} - 1]$, in which case the limits of integration were selected as $t_{x,k}$, $k = 0,1,2,\ldots$. For $x < 10\pi/[4(-y)^{-\frac{1}{2}} - 1]$, the fixed integration step $\Delta t = t_y/5$ (with $\varepsilon_y = 10^{-7}$) was used. For the case $y = 0$, the integrand undergoes 5 oscillations at least before $\operatorname{sech}^{p+1} t$ decreases to $\varepsilon_p = 10^{-6}$ if $x > .125$. Thus, for $y = 0$, the limits of integration were selected as $t_{x,k}$, $k = 0,1,2,\ldots$.

In summary, two cases were considered: (i) for $x < 10\pi/[4(-y)^{-\frac{1}{2}} - 1]$ a fixed integration step $\Delta t = t_y/5$ (with $\varepsilon_y = 10^{-7}$) was used, and

(ii) for $x > 10\pi/[4(-y)^{-\frac{1}{2}}-1]$, the limits of integration were selected as $t_{x,k}$, $k = 0,1,2,\ldots$. In both cases, Simpson's integration rule was used and the integration was pursued until the contribution of the last integration step was less than 10^{-7}. The upper limit of integration was found to vary between about 1 and 4 (except for $x = y = 0$ where it is about 9). The computing time required to evaluate the four wave integrals varied between less than 0.04 sec up to 0.25 sec, representing a cost varying between 0.4¢ up to 2¢.

The numerical calculations were checked against the following results:

$$\Omega c_1(0,0) = 1,\ \Omega c_3(0,0) = 2/3,\ \Omega s_2(0,y) = \Omega s_4(0,y) = 0,$$

$$\Omega c_1(0,y) = \frac{-y}{2} e^{y/2} \left[K_1\left(\frac{-y}{2}\right) - K_o\left(\frac{-y}{2}\right)\right]$$

$$\Omega c_3(0,y) = y\, e^{y/2} \left[\left(1 - \frac{y}{3}\right) K_1\left(\frac{-y}{2}\right) + \frac{y}{3} K_2\left(\frac{-y}{2}\right)\right]$$

$$\Omega c_1(x,0) = \frac{\pi}{2} x \left[\int_o^x Y_o(t)dt - Y_1(x)\right]$$

where Y_o, Y_1, K_o and K_1 are the usual Bessel functions, see Abramowitz and Stegun [7].

The behavior of the four wave integrals Ωc_1, Ωs_2, Ωc_3 and Ωs_4 as functions of $x-\mu$ for $y + \nu = 0$, and as functions of $y + \nu$ for $x-\mu =$ constant, is depicted on Figs. 4.

For large values of x, we may obtain an approximation to these wave integrals by means of the method of stationary phase, see Erdélyi [11]. It is convenient to perform the change of variable $t = \tan\theta$ in (3.20). This yields

$$\Omega_p(x,y) = \int_1^\infty \frac{e^{yt^2}}{t^p(t+1)^{\frac{1}{2}}} \frac{e^{ixt}}{(t-1)^{\frac{1}{2}}}\, dt$$

which is in the form of eq. (4) p. (48) in Erdélyi. We easily obtain

$$\Omega_p(x,y) \sim \left(\frac{\pi}{2}\right)^{\frac{1}{2}} \frac{e^y}{x^{\frac{1}{2}}} e^{i(x+\pi/4)} \left\{1 - i\,\frac{1/4 + p - 2y}{2x} - \frac{3}{8}\,\frac{3 + 24p + 16p^2 + 16y(1-4p+4y)}{16x^2} + \ldots\right\}$$

REFERENCES

1. Gadd, G.E., 1973, "Wave resistance calculations by Guilloton's Method", Trans. RINA, Vol. 115, p. 377.

2. Guilloton, R., 1964, "L'étude théorique du bateau en fluide parfait", ATMA, Vol. 64, p. 537.

3. Dagan, G., 1975, "A method of computing nonlinear wave resistance of thin ships by coordinate straining", to appear in the J. Ship. Res.

4. Noblesse, F., 1975, "A perturbation analysis of the wavemaking of a ship, with an interpretation of Guilloton's method", to appear in the J. Ship Res.

5. Noblesse, F. and Dagan G., 1975, "Nonlinear ship waves theories by continuous mapping", submitted for publication.

6. Wehausen, J.V. and Laitone, E.V., 1960, "Surface waves", Handbuch der Physik, Springer-Verlag, Berlin.

7. Abramowitz, M. and Stegun, I.A., 1964, "Handbook of mathematical functions", Dover, New York.

8. Yeung, R.W., 1972, "Sinkage and trim in first-order thin-ship theory", J.S.R., Vol. 16, p. 47.

9. Hess, J.S. and Smith, A.M.O., 1967, "Calculation of potential flow about arbitrary bodies", Progress in Aeronautical Sciences", Vol. 8, Pergamon Press, New York.

10. Hershey, A.V., 1959, "Computing programs for the complex exponential integral," NPG Report No. 1646, U.S. Naval Proving Ground, Dahlgren, Va.

11. Erdélyi, A. 1956, "Asymptotic expansions", Dover, New York.

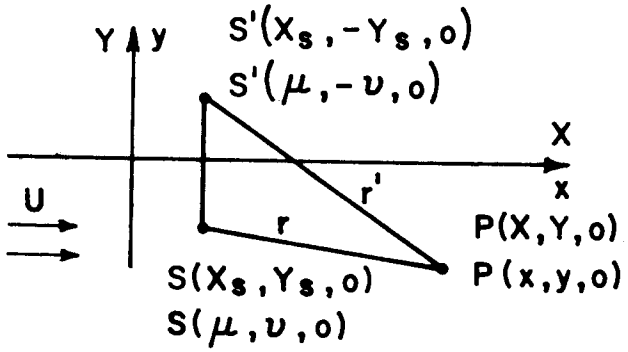

Fig. 1 — Definition sketch for the centerplane Havelock source potential

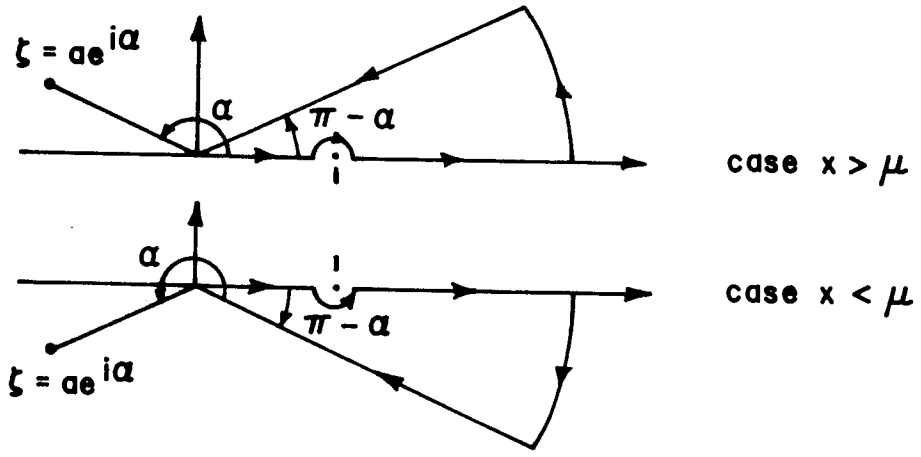

Fig. 2 — Integration contours

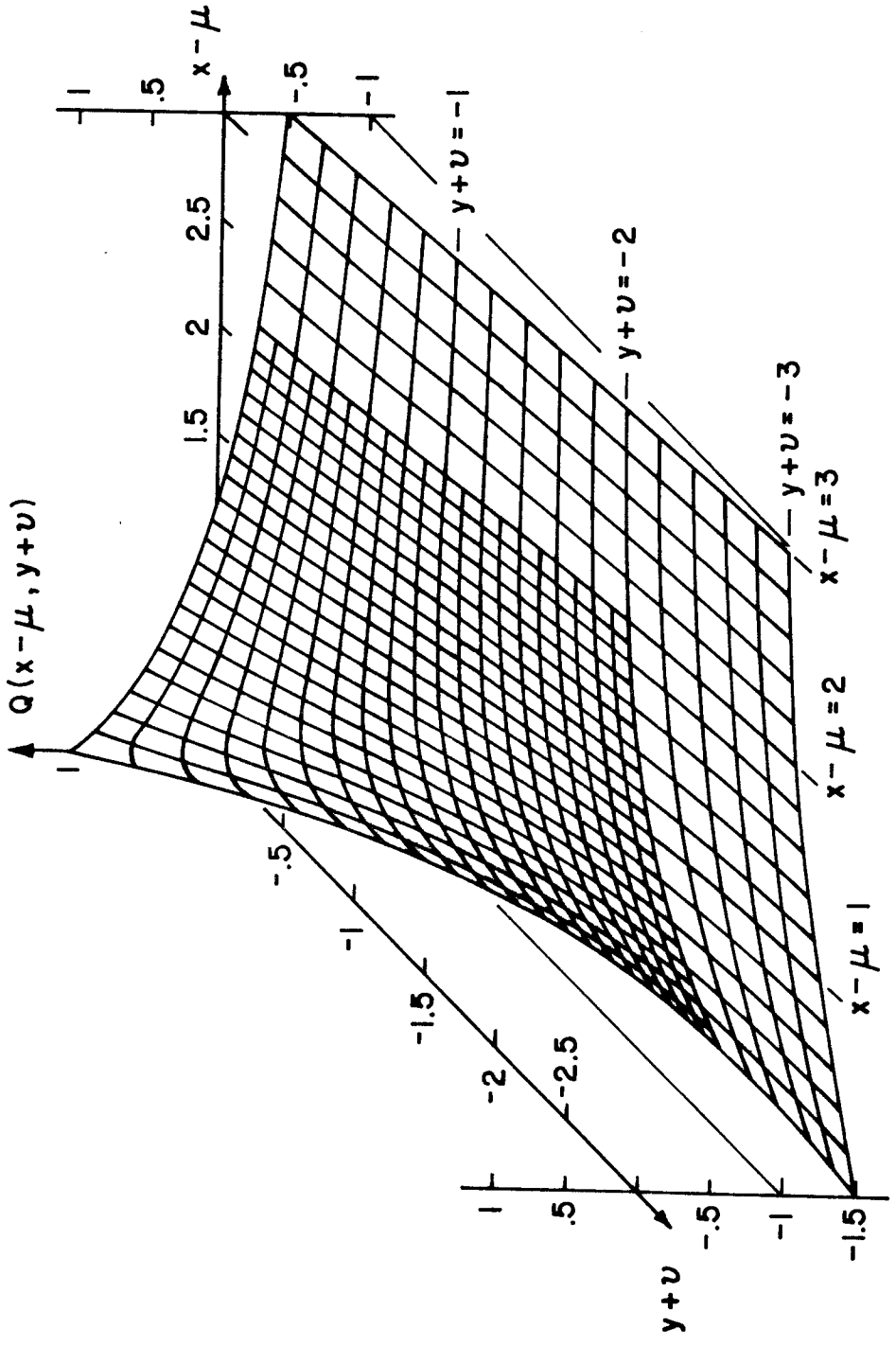

Fig. 3—Strength of the image singularity

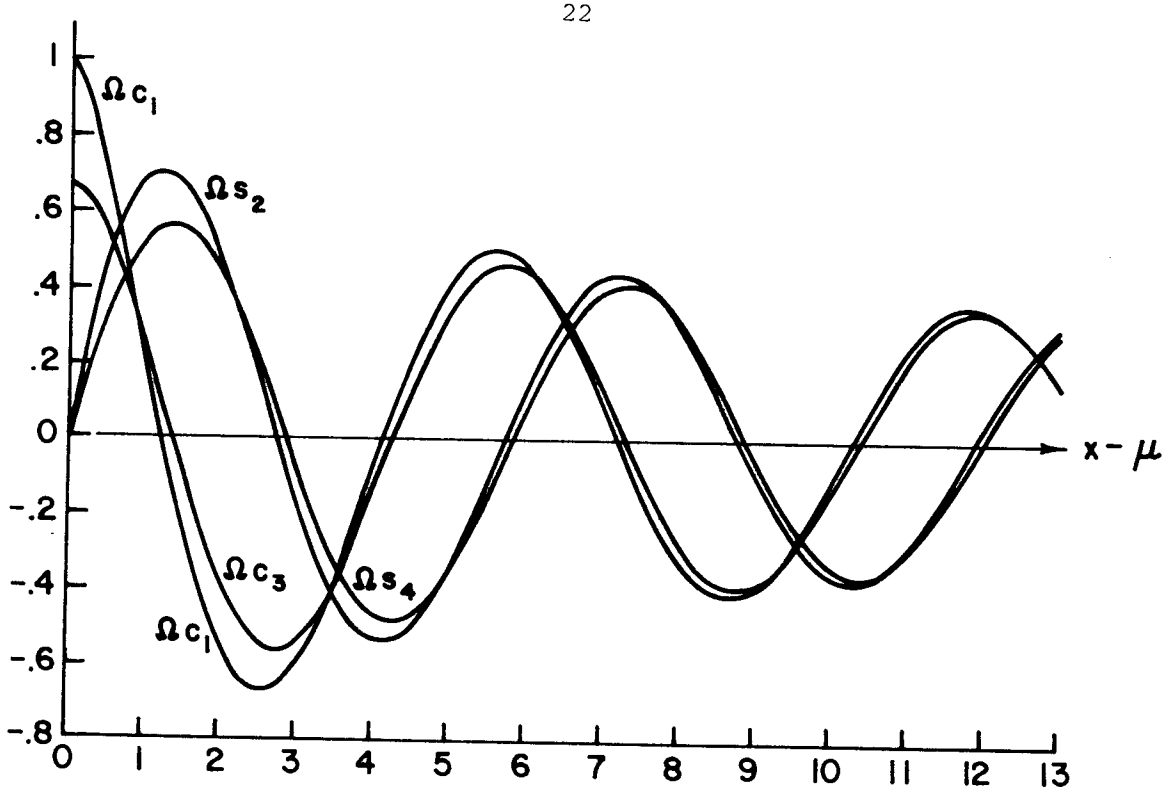

Behavior of the wave integrals as functions of $x-\mu$ for $y+\upsilon=0$

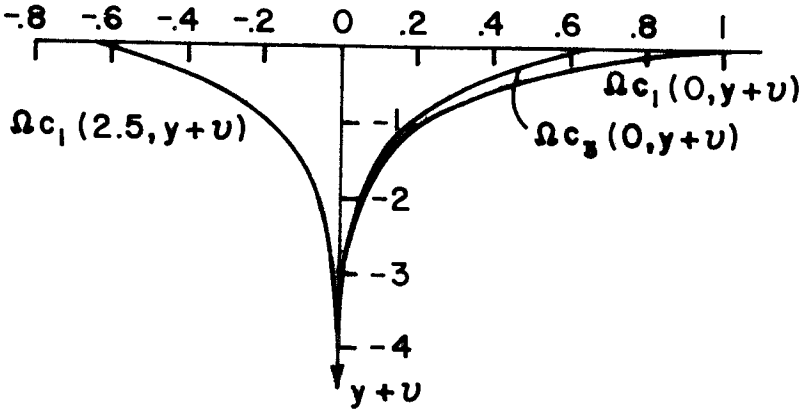

Behavior of the wave integrals as functions of $y+\upsilon$ for $x-\mu=$ constant

Fig. 4 – Wave integrals